Adsorption of reactive dyes onto chitosan/montmorillonite intercalated composite: multi-response optimization, kinetic, isotherm and thermodynamic study

J. Li, J. Cai, L. Zhong, H. Wang, H. Cheng and Q. Ma

ABSTRACT

Chitosan/montmorillonite intercalated composite (CTS/MMT) was used as an effective adsorbent for removal of reactive dyes, i.e. Reactive Black 5 (RB5), Reactive Red 136 (RR136), Reactive Yellow 145 (RY145) and Reactive Blue 222 (RB222). Taguchi method attached grey relational analysis was applied to determine the optimal adsorption conditions, including pH, initial concentration of dye, temperature, adsorbent dosage and contact time, for achieving simultaneous maximization of removal percentage and adsorption capacity. The percentage contribution of each adsorption condition was determined in the analysis of variance and showed that the most effective parameter in removal of RB5, RY145 and RB222 is the dye solution pH, whereas the initial concentration was the determining factor for optimum efficiency for the dye RR136. Under respective optimal condition, the removal percentages and adsorption capacity of four reactive dyes onto CTS/MMT were both found in the following order: RR136 > RY145 > RB5 > RB222. The maximum removal percentages of 78.8 and 49.5%, and the adsorption capacity of 315.20 and 123.75 mg/g were obtained for RR136 and RB222, respectively. The adsorption behaviors showed that the adsorption kinetics and isotherms were in best agreement with Avrami fractionary order model and the Toth isotherm, respectively.

Key words | adsorption, chitosan, grey relational analysis, montmorillonite, reactive dyes, Taguchi method

J. Li (corresponding author)
Q. Ma
Key Laboratory of Marine Environment & Ecology, Ministry of Education,
Ocean University of China,
Qingdao 266100,
China
E-mail: *lijin@ouc.edu.cn*

J. Cai
Key Laboratory of Fermentation Engineering, Ministry of Education,
Hubei University of Technology,
Wuhan 430068,
China

L. Zhong
College of Chemistry and Chemical Engineering,
Ocean University of China,
Qingdao 266100,
China

H. Wang
H. Cheng
College of Environmental Science and Engineering,
Ocean University of China,
Qingdao 266100,
China

NOMENCLATURE

A_T Temkin isotherm equilibrium binding constant (L/g)
B_{DR} Dubinin-Radushkevich isotherm constant (mol^2/J^2)
b_T Temkin isotherm constant related to the heat of adsorption (J/mol)
C_P constant related with the thickness of boundary layer (mg/g)
C_0 initial adsorbate concentration in liquid phase (mg/L)
C_e liquid phase adsorbate concentration at equilibrium (mg/L)
C_f final adsorbate concentration in liquid solution (mg/L)
C_t adsorbate concentrations at contact time t (mg/L)
E_{DR} the mean-free energy of the adsorption (J/mol)
ΔG^0 Standard Gibbs free energy change (kJ/mol)
ΔH^0 Standard free enthalpy change (kJ/mol)
k_1 pseudo-first-order kinetic model constant (min^{-1})
k_2 pseudo-second-order kinetic model constant (g/(mg min))
k_{Av} Avrami kinetic model constant (min^{-1})
k_p intra-particle diffusion kinetic model constant ($mg/(g\ min^{1/2})$)
K_F Freundlich isotherm constant related to the adsorption capacity $(mg/g)(L/mg)^{1/n}$
K_L Langmuir isotherm constant (L/mg)
K_{LF} Langmuir-Freundlich isotherm constant (L/mg)
K_S Sips isotherm constant (L/mg)
K_T Toth isotherm constant (L/mg)
m adsorbent dosage (g)
m_{LF} Langmuir-Freundlich model exponent
n Freundlich constant related to adsorption intensity
n_{Av} Avrami exponent related to the adsorption mechanism

doi: 10.2166/wst.2018.221

n_S Sips model exponent
q adsorption capacity obtained from Taguchi experiment (mg/g)
q_e adsorption capacity at equilibrium (mg/g)
$q_{e,cal}$ calculated adsorption capacity at equilibrium (mg/g)
$q_{e,exp}$ experimental adsorption capacity at equilibrium (mg/g)
q_m the maximum adsorption capacity predicted by isotherms (mg/g)
q_t adsorption capacity at time t (mg/g)
R ideal gas constant (8.314 J/mol K)
R^2 coefficient of determination
R_L Langmuir separation factor
ΔS^o standard free entropy change (kJ/(mol K))
t Toth isotherm constant
T absolute temperature (K)
V volume of the adsorbate solution (L)

Greek letters

α initial adsorption rate constant of Elovich-chemisorption model (mg/(g min))
β Elovich constant related to the extent of surface coverage and activation energy involved in chemisorption (g/mg)
ε Polanyi potential

Symbols

A pH of dye solution in the Taguchi experiment
B initial concentration of dye in the Taguchi experiment (mg/L)
C temperature in the Taguchi experiment (°C)
D adsorbent dosage in the Taguchi experiment (g/L)
E contact time in the Taguchi experiment (min)

INTRODUCTION

In recent years, reactive dyes have been extensively used in textile, leather, paper and cosmetic industries due to their bright colors and excellent color fastness. It is estimated that up to 50% of reactive dyes may be lost to the effluents during the dyeing process (Blackburn 2004). Reactive dyes, when launched into the ecosystem without any previous treatment, not only involve aesthetic pollution, but cause damage to the ecological balance since their molecules may show carcinogenic properties or mutagenic actions on living organisms (Oliveira *et al.* 2011). Therefore, the removal of reactive dyes from waste effluents before they are discharged to natural water bodies becomes environmentally important.

Due to the presence of azo groups in cooperation with substituted aromatic structures, reactive dyes show high resistance to oxidation, light, and poor biodegradability. Hence, physical methods, especially adsorption on low cost, non-toxic and readily available adsorbents have been considered a comparatively simple, effective and economical process for the removal of reactive dyes from wastewater that avoids generation of toxic secondary degradation by products (Zhao *et al.* 2017).

Chitosan (CTS) is the *N*-deacetylated derivative of chitin and the second most plentiful natural biopolymer. As a well-known adsorbent, CTS has exhibited a higher adsorption capacity of dye than activated carbon. The presence of amino, acetamide and hydroxyl functional groups in CTS molecular chains serve as the active sites for adsorption. However, the application of chitosan as adsorbents in either batch or column modes is limited because of its unfavorable mechanical property (due to its extensive hydrophilicity and pH sensitivity), the low specific gravity and relative high market cost.

Another kind of attractive adsorbent is montmorillonite (MMT) due to its natural abundance, low cost, high surface area, high-cation exchange capacity and a layered structure which can act as host materials with excellent adsorption properties. Although montmorillonite possess the high adsorption capabilities, the modification of their structure can successfully improve their capabilities.

Chitosan/montmorillonite intercalation composite (CTS/MMT) has attracted great interest because it often exhibits remarkable improvement in materials properties when compared with virgin chitosan and montmorillonite, or other conventional micro- and macro-composites (Alexandre & Dubois 2000). And they, as adsorbents, are drawing more and more attention due to their high specific surface area, chemical and mechanical stability, and variety of surface and structural properties (Monvisade & Siriphannon 2009).

During adsorption process of reactive dyes, not only adsorbents characteristics play a major role, but the operational variables, such as pH, dye concentration, temperature, adsorbent dosage and contact time dramatically affect the adsorption efficiency. In order to attain the maximum removal efficiency of reactive dyes, an optimization strategy is required to find the best experimental condition

(Zolgharnein *et al.* 2014). From an economic and environmental viewpoint, determining the optimal experimental conditions that simultaneously maximize the removal percentage ($R\%$) and adsorption capacity (q) is quite favorable. The highest $R\%$ with the least amount of adsorbent usage is favorable because high $R\%$ guarantees satisfactory decontamination of the solution and high q avoids exceeding waste production.

Taguchi optimization technique, based on orthogonal array of experiments, has been generally adopted to optimize the design variables because it can significantly minimize the overall experimental time and costs (Zolgharnein *et al.* 2013), but it is not suitable for optimization of multi-response optimization problem. Grey relational analysis (GRA), based on grey system theory, is suitable for solving problems with complicated interrelationships between multiple factors and variables. The combination of the Taguchi method and GRA is a practical and efficient approach in solving multi-response optimization problems.

The present study was focused on the application of CTS/MMT for the removal of reactive dyes from aqueous solution with the purpose to multi-response optimize the best adsorption conditions on the basis of Taguchi design attached with GRA. Four kinds of reactive dyes, i.e. Reactive Black 5 (RB5), Reactive Red 136 (RR136), Reactive Yellow 145 (RY145) and Reactive Blue 222 (RB222), were selected as model reactive dyes. Furthermore, kinetic studies, isotherm modeling and thermodynamic studies of reactive dyes adsorption were comprehensively investigated.

METHODS

Materials

Chitosan (CTS) with a degree of deacetylation (DD) of 86% and a weight-average molecular weights (M_w) of 328 kDa was obtained from Shandong Aokang Biotechnology Co. (Shandong, China). Montmorillonite (MMT) was purchased from Zhejiang Sanding Technology Co., Ltd (Shaoxing, China) and the cation exchange capacity (CEC) was 0.9 mmol/g.

Four kinds of reactive dyes, namely RB5, RR136, RY145 and RB222, were obtained from a textile company and the molecular structure and some characteristics were displayed in Table 1. Reactive dyes, in commercial purity, were used without further purification.

All other reagents were analytical grade and used as received. Herein, NaOH or HCl (0.1 mol/L) was used to adjust the pH of the dye solutions. Deionized water was used in all experiments.

Preparation of CTS/MMT

CTS/MMT was prepared according to Wang *et al.* (2008) and modified as follows: 4.0 g of MMT was swelled by 100 mL distilled water. 3.3 g CTS was prepared by dissolving in 1% (v/v) CH_3COOH solution, and then the pH of the resulting solution was adjusted to 4.9 with 5 mol/L NaOH solution. Next, CTS solution was slowly added to MMT suspension followed by stirring at 60 °C for 6 h to obtain composite. The formed composite was washed with distilled water until the pH of the supernatant reached 7. The composite was collected after being dried at 60 °C to get sample CTS/MMT.

Adsorption experiments

Two types of adsorption experiments were performed in this study. The first type was carried out for the sixteen different experiments using $L_{16}(4^5)$ orthogonal array obtained by the Taguchi experimental design. In each experiment, 50 mL reactive dye solutions with different pH, initial concentrations and adsorbent dosage were put into a thermostated shaker rotated at 150 rpm. After shaking for an predetermined time at a predetermined temperature, the solutions were filtered and the supernatant was collected for the determination of final dye concentration at the maximum wavelength, λ_{max}, as shown in Table 1. The $R\%$ and q, the two objective functions need to be maximized by Taguchi method, were calculated according to the following equations:

$$R\% = \frac{C_0 - C_f}{C_0} \times 100 \quad (1)$$

$$q = \frac{(C_0 - C_f)V}{m} \quad (2)$$

The second type of adsorption experiments were carried out to obtain the adsorption kinetics and isotherms. The kinetic experiments were carried out for different contact times while reactive dyes concentration (200 mg/L) and adsorbent dosage (0.4 g/L) were kept constant. The rest of the adsorption conditions were selected according to the results of the Taguchi-GRA. At various time intervals, the residual concentration of dye in the solution was measured. The

Table 1 | Structure and characteristics of the four reactive dyes as adsorbate in the present study

C.I. generic name	Structure	λ_{max} (nm)	Chemical type
Reactive Black 5 (RB5)	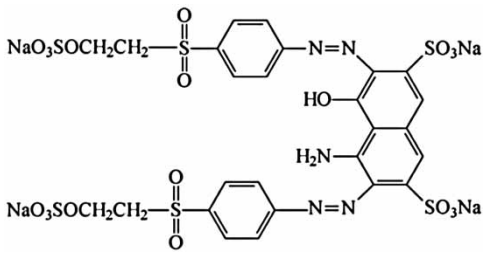	600	Diazo
Reactive Red 136 (RR136)	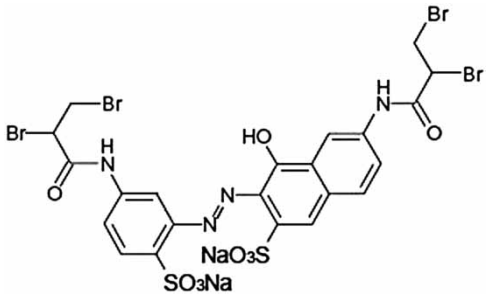	510	Monoazo
Reactive Yellow 145 (RY145)	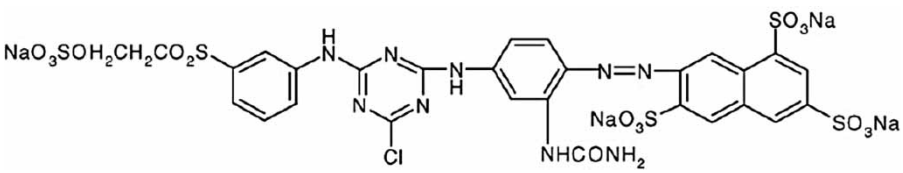	420	Monoazo
Reactive Blue 222 (RB222)	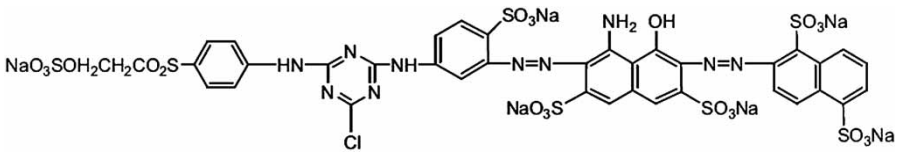	610	Diazo

adsorption capacity at time t, q_t (mg/g), was calculated by:

$$q_t = \frac{(C_0 - C_t)V}{m} \tag{3}$$

The adsorption isotherm studies were performed following a similar procedure: reactive dye solution with different initial concentrations ranging from 50 to 400 mg/L were used and the equilibrium time was set as 240 min, which was enough according to the preliminary experiments. The adsorbent dosage was fixed at 0.4 g/L. The adsorption capacity at equilibrium, q_e (mg/g), was calculated by:

$$q_e = \frac{(C_0 - C_e)V}{m} \tag{4}$$

The experiments were conducted in triplicate and the negative controls (without adsorbent) were simultaneously performed to ensure that adsorption was not by the container but by the adsorbent.

Taguchi-GRA multi-response optimization

Taguchi experimental design

$L_{16}(4^5)$ orthogonal array was used for the experimental design in order to achieve the optimization adsorption process. The five selected factors, including pH, initial concentration of dye, temperature, adsorbent dosage, and contact time, along with their levels (four levels for each factor) are listed in Table 2.

Taguchi uses the S/N ratio to measure the response characteristic deviating from the desired value. Log functions of the S/N ratio serve as the objective functions for optimization. The maximum R% and q are required in the

Table 2 | Controllable factors and their levels used in the Taguchi experimental design

Factor	Description	Level 1	Level 2	Level 3	Level 4
A	pH	3	4	5	6
B	Initial concentration of dye (mg/L)	50	100	200	300
C	Temperature (°C)	20	30	40	50
D	Adsorbent dosage (g/L)	0.4	0.5	0.6	0.7
E	Contact time (min)	60	120	180	240

present study; *S/N* ratio analysis following Equation (5) for the 'larger is better' (LIB) category is applied for selection of the optimum condition:

$$\frac{S}{N} = -10\log\left(\frac{1}{n}\sum_{i=1}^{n}\frac{1}{y_i^2}\right) \tag{5}$$

where n is the number of observations and y is the observed response (R% and q).

Grey relational analysis

GRA is used to convert the optimization problem from a multi-response to a single-response. This analysis consists of the following steps.

First, the *S/N* ratios obtained from the Taguchi method are normalized from 0 to 1 according to Equation (6):

$$Z_{ij} = \frac{y_{ij} - \min y_{ij}}{\max y_{ij} - \min y_{ij}} \tag{6}$$

where Z_{ij} is the normalized *S/N* value for ith trial for jth dependent response, and y_{ij} is *S/N* ratio obtained from experiments, miny_{ij} and maxy_{ij} are the minimum and maximum values of *S/N* value obtained for each experiment, respectively.

Second the grey relational coefficient (*GRC*) from the normalized *S/N* ratio values is computed according to the following:

$$GRC_{ij} = \frac{\Delta_{\min} + \psi\Delta_{\max}}{\Delta_{ij} + \psi\Delta_{\max}} \tag{7}$$

where Δ_{ij} is the absolute difference between y_{0j} and y_{ij}. y_{0j} and y_{ij} are the ideal normalized value and ith normalized value of the jth response. Δ_{min} and Δ_{max} are the minimum and maximum values of Δ_{ij}. ψ is the distinguishing coefficient and was taken as 0.5 in this study.

Third, the grey relational grade (*GRG*) is computed by the following equation:

$$GRG_{ij} = \frac{1}{n}\sum GRC_{ij} \tag{8}$$

where n is the number of responses; in this study, n is 2.

Fourth, performance prediction and confirmation test are carried out. The predicted GRG_p with optimal parameters can be computed as the following equation:

$$GRG_p = GRG_m + \sum_{i=1}^{n}(GRG_o - GRG_m) \tag{9}$$

where GRG_m and GRG_o are the overall mean and individual *GRG* at the optimal level, respectively, and n is the number of the operational variables.

Finally, analysis of variance (ANOVA) is used to estimate the contribution of each factor on *GRG*.

All data processing, including the design of experiments, ANOVA, and optimization of the process were done by Qualitek-4 statistical software.

Error analysis

Kinetic and isotherm models were modeled by a non linear regression method using a trial-and-error procedure of the solver add-in with Microsoft Excel. The coefficient of determination (R^2) and the nonlinear chi-square test (χ^2) were used to test the best fit of the kinetic and isotherm model to the experimental data, as shown in the following equation:

$$R^2 = \frac{\sum(q_{cal} - \overline{q_{\exp}})^2}{\sum(q_{cal} - \overline{q_{\exp}})^2 + \sum(q_{cal} - q_{\exp})^2} \tag{10}$$

$$\chi^2 = \sum\frac{(q_{\exp} - q_{cal})^2}{q_{cal}} \tag{11}$$

An R^2 value closer to one and a smaller χ^2 value indicate the data from kinetic and isotherm models are similar to the experimental data.

Thermodynamic studies

The standard Gibbs free energy change (ΔG^o) is calculated from the relationship at different temperatures under optimum conditions obtained from Taguchi-GRA:

$$\Delta G^o = -RT\ln K_d \tag{12}$$

The thermodynamic equilibrium constant, K_d, can be calculated by the method suggested by Boparai *et al.* (2011).

The adsorption isotherm data were plotted as $\ln(q_e/C_e)$ versus q_e, and then a linear regression was performed based on least-squares analyses and the intercept on the y-axis gives the value of $\ln K_d$.

The corresponding standard enthalpy changes (ΔH^o) and standard entropy changes (ΔS^o) can be obtained from the slope and intercept from the Van 't Hoff plot according to the equation (Liang *et al.* 2013):

$$\ln K_d = \frac{\Delta S^o}{R} - \frac{\Delta H^o}{RT} \tag{13}$$

RESULTS AND DISCUSSION

Multi-response optimization using Taguchi-GRA

The objective of applying Taguchi-GRA multi-responses optimization is to determine the optimum adsorption conditions at which R% and q are maximized simultaneously. The highest R% with the least amount of adsorbent is quite favorable from an environmental and economical viewpoint, because high R% guarantees satisfactory decontamination of the solution and high q avoids excess waste production (Zolgharnein *et al.* 2013, 2014).

In the Taguchi method, orthogonal array design is planned to study the entire operational variables with a small number of experiments only. The R% and q were selected as two response variables. The mean S/N ratio of R% and q for each level of the operational variables calculated according to Equation (5) are given in Table 3. Regardless of the category of the operational variables, a larger S/N ratio corresponds to better operational variables and the optimum level is determined from the highest value. As shown in Table 3, for RR136, the mean S/N ratio of R% was maximized under the conditions given for experiment number 3, while the mean S/N ratio of q was maximized under the conditions given for experiment number 12. For the other three kinds of reactive dyes, the mean S/N ratios of R% were maximized under the conditions given for experiment number 5, while the mean S/N ratios of q were maximized under the conditions given for experiment number 4. It is obvious that there is a great inconsistency of operational variables for achieving optimization of two different objective functions, so the traditional Taguchi method is not suitable for the problem with multi-response characteristics.

According to the GRA, the normalized S/N ratios values in the range of 0 to 1 obtained from Equation (6) are given in Table 3. Then *GRC* were calculated using Equation (7) from the normalized S/N ratio to express the relationship between the ideal and the actual normalized S/N ratio. The overall evaluation of the multi-response is based on the *GRG*, which is computed by averaging the *GRC* corresponding to each response according to Equation (8). The *GRG* indicates the degree of influence that a comparability sequence could exert over the reference sequence. Therefore, if a particular comparability sequence is more important than the other ones to the reference sequence, then the *GRG* for that comparability sequence will be higher than other *GRG*. The *GRC* and *GRG* with their rank of all the experiments are represented in Table 4. As shown in Table 4, the multi-response optimization problem has been converted into a unique equivalent objective function optimization problem using the combination of Taguchi and GRA. For RR136, experiment number 3, for which the combination condition was $A_1B_3C_3D_3E_3$, had the best multi-response characteristics among the 16 experiments because it corresponds to the highest *GRG*. For the other three kinds of reactive dyes, experiment number 4, for which the combination condition was $A_1B_4C_4D_4E_4$, had the best multi-response characteristics.

For the orthogonal experimental design, it is possible to separate out the effect of each operational variable at different levels. Since the mean *GRG* represents the level of correlation between the comparability sequence and the reference sequence, the greater the value of the mean *GRG*, the stronger the correlation to the reference sequence. Therefore, the optimal level of each factor is the level with the highest value of the mean *GRG*. The mean *GRG* values for each level are summarized in Figure 1, in which the optimum levels are highlighted in circles.

According to the optimal level of each factor, the predicted optimal combination adsorption conditions and predicted *GRG*, which were obtained from the simulation at optimum level obtained from Figure 1, are listed in Table 5. It was revealed that RB5 and RY145 showed the highest *GRG* at the same adsorption conditions in the initial experiment, as in experiment number 4, for which the combination condition was $A_1B_4C_4D_4E_4$. For RR136 and RB222, as none of the experiments fitted the optimal adsorption conditions, an experiment was conducted as a predicted run. The results shown in Table 5 indicated that there was a good agreement between the predicted and experimental results. For RR136, compared with the initial adsorption conditions (shown in Table 4), $A_1B_3C_3D_3E_3$, which showed the highest *GRG* as 0.895, the predicted optimal combination adsorption conditions, $A_1B_3C_1D_2E_3$, showed the higher *GRG* as 0.984. The results indicated that the

Table 3 | Mean *S/N* ratio with their normalized value for removal percentage (*R*%) and adsorption capacity (*q*)

	RB5				RR136				RY145				RB222			
	Mean *S/N* ratio		Normalized *S/N* ratio		Mean *S/N* ratio		Normalized *S/N* ratio		Mean *S/N* ratio		Normalized *S/N* ratio		Mean *S/N* ratio		Normalized *S/N* ratio	
Trial no.	*R*%	*q*	*R*%	*q*	*R*%	*q*	*R*%	*q*	*R*%	*q*	*R*%	*q*	*R*%	*q*	*R*%	*q*
1	31.91	33.85	0.422	0.168	36.24	44.76	0.738	0.497	33.75	35.69	0.476	0.195	32.88	34.82	0.822	0.306
2	34.26	40.28	0.700	0.524	37.12	49.16	0.926	0.754	35.71	41.74	0.822	0.552	33.54	39.56	0.894	0.669
3	34.73	45.19	0.755	0.796	37.46	51.09	1	0.867	36.21	46.67	0.910	0.843	31.50	41.96	0.670	0.853
4	36.23	48.87	0.932	1	35.20	49.74	0.515	0.788	36.68	49.32	0.993	1	31.25	43.89	0.642	1
5	36.80	35.22	1	0.244	36.65	40.73	0.825	0.261	36.72	35.14	1	0.163	34.49	32.91	1	0.160
6	34.26	37.36	0.700	0.362	37.10	45.62	0.923	0.547	35.18	38.27	0.727	0.348	33.13	36.22	0.849	0.414
7	33.22	47.20	0.577	0.908	34.69	52.75	0.405	0.964	34.39	48.37	0.588	0.944	29.56	43.54	0.455	0.973
8	32.02	47.59	0.435	0.929	34.36	52.43	0.335	0.945	33.43	49.00	0.420	0.981	27.33	42.89	0.209	0.924
9	33.74	30.81	0.638	0	33.76	36.26	0.206	0	35.31	32.38	0.750	0	33.74	30.82	0.917	0
10	32.39	36.83	0.479	0.333	34.92	45.02	0.454	0.512	33.87	38.30	0.496	0.350	32.12	36.56	0.738	0.439
11	32.80	44.84	0.527	0.777	36.73	52.30	0.843	0.938	33.11	45.15	0.363	0.754	28.65	40.70	0.355	0.756
12	31.23	48.73	0.342	0.992	32.80	53.36	0	1	31.37	48.87	0.056	0.973	25.43	42.94	0	0.927
13	31.88	31.88	0.419	0.059	33.28	39.30	0.103	0.178	35.47	35.47	0.779	0.182	32.93	32.93	0.827	0.162
14	31.96	39.92	0.428	0.504	33.74	48.28	0.201	0.703	32.09	40.05	0.183	0.453	32.18	40.14	0.745	0.713
15	28.73	37.85	0.047	0.390	33.59	45.63	0.168	0.548	31.90	41.02	0.150	0.510	28.64	37.76	0.354	0.531
16	28.33	42.31	0	0.637	35.05	51.17	0.482	0.872	31.05	45.03	0	0.747	25.79	39.76	0.039	0.684

Table 4 | Grey relational coefficient (*GRC*) with their grade (*GRG*) and rank for removal percentage (*R*%) and adsorption capacity (*q*)

	RB5				RR136				RY145				RB222			
	GRC				*GRC*				*GRC*				*GRC*			
Trial no.	*R*%	*q*	*GRG*	Rank	*R*%	*q*	*GRG*	Rank	*R*%	*q*	*GRG*	Rank	*R*%	*q*	*GRG*	Rank
1	0.354	0.358	0.420	14	0.656	0.499	0.577	10	0.488	0.383	0.436	15	0.737	0.419	0.578	11
2	0.604	0.505	0.569	8	0.871	0.670	0.771	3	0.737	0.527	0.632	7	0.826	0.601	0.714	2
3	0.753	0.702	0.691	5	1.000	0.790	0.895	1	0.848	0.762	0.805	2	0.602	0.772	0.687	4
4	1.000	0.915	0.940	1	0.508	0.702	0.605	9	0.986	1.000	0.993	1	0.583	1.000	0.791	1
5	0.635	0.370	0.699	3	0.741	0.404	0.572	11	1.000	0.374	0.687	5	1.000	0.373	0.687	4
6	0.569	0.434	0.532	9	0.867	0.525	0.696	4	0.647	0.434	0.540	9	0.768	0.460	0.614	8
7	0.572	0.815	0.693	4	0.456	0.933	0.695	5	0.548	0.898	0.723	3	0.478	0.949	0.714	2
8	0.466	0.826	0.673	6	0.429	0.901	0.665	7	0.463	0.963	0.713	4	0.387	0.868	0.628	7
9	0.490	0.333	0.457	12	0.386	0.333	0.360	16	0.667	0.333	0.500	11	0.857	0.333	0.595	10
10	0.412	0.415	0.459	11	0.478	0.506	0.492	13	0.498	0.435	0.466	13	0.656	0.471	0.564	12
11	0.552	0.694	0.603	7	0.761	0.889	0.825	2	0.440	0.670	0.555	8	0.437	0.672	0.554	14
12	0.478	1.000	0.708	2	0.333	1.000	0.667	6	0.346	0.949	0.648	6	0.333	0.873	0.603	9
13	0.374	0.341	0.405	15	0.358	0.378	0.368	15	0.693	0.379	0.536	10	0.743	0.374	0.558	13
14	0.412	0.485	0.484	10	0.385	0.627	0.506	12	0.380	0.477	0.429	16	0.662	0.636	0.649	6
15	0.333	0.465	0.397	16	0.375	0.525	0.450	14	0.370	0.505	0.438	14	0.436	0.516	0.476	16
16	0.355	0.623	0.456	13	0.491	0.796	0.644	8	0.333	0.664	0.498	12	0.342	0.613	0.478	15

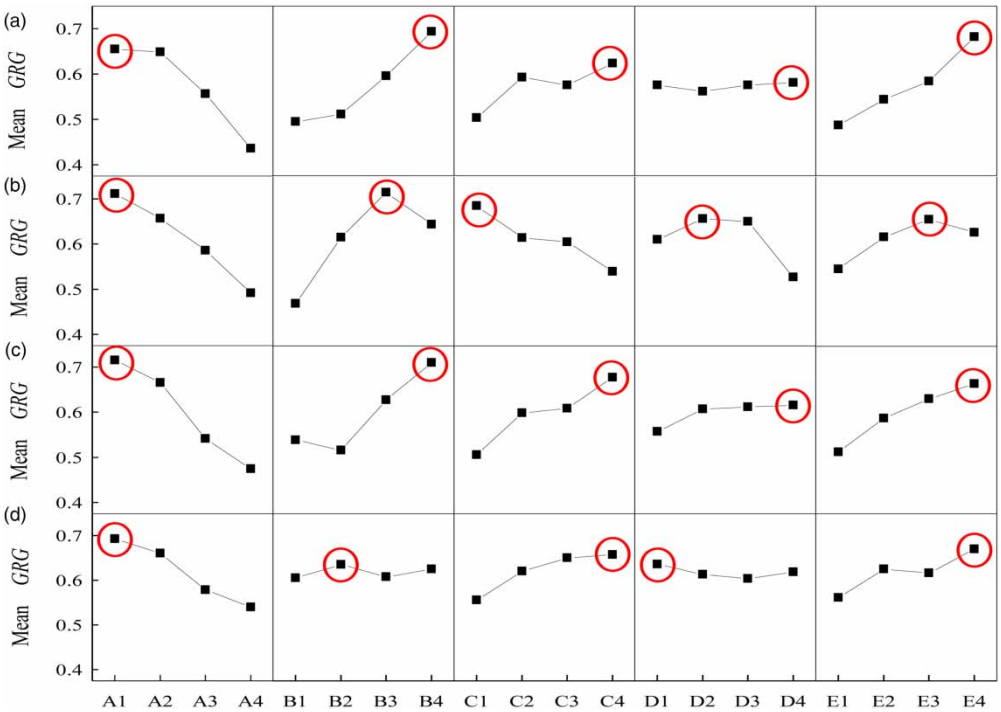

Figure 1 | Main effect plots showing the effect of control factors on the response variable grey relational grade (*GRG*). (a) Reactive Black 5, (b) Reactive Red 136, (c) Reactive Yellow 145, and (d) Reactive Blue 222. A: pH, B: initial concentration of dye (mg/L), C: temperature (°C), D: adsorbent dosage (g/L), E: contact time (min). The levels are as shown in Table 2.

Table 5 | Confirmation test results for multi-response with initial and optimal adsorption conditions

	Initial condition				Optimal condition				
					Prediction		Confirmation test		
Reactive dye	Level	*R* (%)	*q* (mg/g)	*GRG*	Level	GRG_P	*R* (%)	*q* (mg/g)	*GRG*
RB5	$A_1B_4C_4D_4E_4$	64.8	277.59	0.940	$A_1B_4C_4D_4E_4$	0.940	64.8	277.59	0.940
RR136	$A_1B_3C_3D_3E_3$	74.7	358.40	0.895	$A_1B_3C_1D_2E_3$	0.980	78.8	315.20	0.984
RY145	$A_1B_4C_4D_4E_4$	68.3	292.55	0.993	$A_1B_4C_4D_4E_4$	0.993	68.3	292.55	0.993
RB222	$A_1B_4C_4D_4E_4$	36.5	156.48	0.791	$A_1B_2C_4D_1E_4$	0.818	49.5	123.75	0.825

adsorption process can be improved due to lower temperature and adsorbent dosage. For RB222, compared with the initial adsorption conditions (shown in Table 4), $A_1B_4C_4D_4E_4$, which showed the highest *GRG* as 0.791, the predicted optimal combination adsorption conditions, $A_1B_2C_4D_1E_4$, showed the higher *GRG* as 0.825. The results indicated that the adsorption process can be improved due to lower initial concentration of dye solution and adsorbent dosage. It also can be concluded from Table 5, for RR136 and RB222, the optimum condition improved *R*% at the cost of reducing limited *q*. The *R*% and *q* for four kinds of reactive dyes were found in the following order under their respective optimal combination condition: RR136 > RY145 > RB5 > RB222. Because the same adsorbent CTS/MMT was used in this study, the variability of adsorption efficiency for four kinds of reactive dyes could be attributed to the different size and chemical structure of the reactive dyes.

In order to investigate which factor significantly influences the multi-response characteristics in most, ANOVA was carried out on the *GRG* values and the contribution percentages of each factor are shown in Figure 2. It is observed that the significant factor was initial concentration for RR136 and dye solution pH for the other three kinds of reactive dyes, respectively. For RB5 and RY145, pH influences most on the multi-response adsorption process followed by initial concentration of dye solution while adsorbent dosage was the smallest contribution. For RB222, pH influenced the multi-response process above 50% followed by contact time and

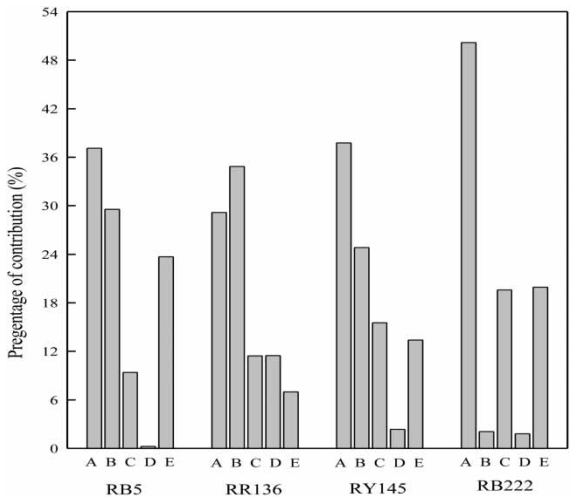

Figure 2 | Percentage of contribution of factors for grey relational grade (*GRG*). A: pH, B: initial concentration of dye (mg/L), C: temperature (°C), D: adsorbent dosage (g/L), E: contact time (min).

temperature, while initial concentration of dye solution and adsorbent dosage influenced very limited. For RR136, the significant factor was initial concentration of dye solution followed by the pH of dye solution.

Adsorption kinetic

The adsorption process of a solute by a solid in aqueous solution is complex. Adsorption kinetic studies can provide valuable information about the mechanism of the adsorption process, which is important for optimizing the adsorption process. In order to investigate the adsorption mechanism and potential rate controlling step, five common kinetic models including Avrami fractionary order, pseudo-first order, pseudo-second order, Elovich and intra-particle diffusion depicted in Table 6 were employed to describe the adsorption process of reactive dyes on CTS/MMT.

Parameters of kinetic models, R^2 and χ^2 are shown in Table 7. As shown in Table 7, in the case of Avrami fractionary order, pseudo-first order and pseudo-second order, Avrami fractionary order exhibited the best-fit for all four kinds of reactive dyes, presenting lowest χ^2 (<0.057) and highest R^2 (>0.9996). In addition, the $q_{e,cal}$ values calculated according to Avrami fractionary order were closest to the experimental $q_{e,exp}$ values, when compared with the other kinetic models. These results indicated that Avrami fractionary order kinetic model was suitable for explanation of the adsorption process of reactive dyes onto CTS/MMT. The Avrami exponential, n_{Av}, is a fractionary number related with the possible changes of the adsorption mechanism that takes place during the adsorption process (Lopes *et al.* 2003). As shown in Table 7, the low magnitude of n_{Av}, in the range of 0.682 and 0.750, suggested that adsorption does not occur with constant growth rate and adsorption process involved more than one reaction pathway (Cestari *et al.* 2006), such as electrostatic, chemical and physical adsorption between reactive dye molecules and the active site on CTS/MMT (Lopes *et al.* 2003). RR136 presented the relatively lowest n_{Av} value when compared with the other absorbates, which suggests its level of the adsorption kinetic order is lower than the others.

Except Avrami fractionary order, the pseudo-second-order kinetic model also showed satisfactory fit with experimental data ($\chi^2 < 0.225$ and $R^2 > 0.9984$), and indicated that it can be used to describe the adsorption process. This phenomenon may be attributed to the fact that the pseudo-second-order kinetic model described the total adsorption process, consisting of external fluid film diffusion, intra-particle diffusion, and surface adsorption (Ho & McKay 1999).

The kinetic data were also analyzed using Elovich model, which is based on a general second-order reaction mechanism for heterogeneous adsorption processes. As shown in Table 7, the Elovich kinetic model did not exhibit a good fit with experimental data ($R^2 < 0.9746$ and $\chi^2 > 3.731$) compared to Avrami fractionary order and pseudo-second-order model, which indicated that the Elovich model cannot be used to describe the kinetics of adsorption process (Ho & McKay 1998). The values of the desorption rate constant, β, related to the extent of surface coverage and activation energy for chemisorptions, were very small, ranging between 0.0175 and 0.0137 g/mg, for all four kinds of reactive dyes. These values indicated a low desorption rate, leading to the conclusion that there is an effective interaction between reactive dyes and CTS/MMT, and the adsorption of reactive dyes onto CTS/MMT is almost irreversible.

For intra-particle diffusion, if intra-particle diffusion occurs, then q_t versus $t^{1/2}$ will be linear. And if the plot passes through the origin, then the rate limiting process is only due to the intra-particle diffusion. Otherwise, some other mechanism along with intra-particle diffusion is also involved. As shown in Table 7, the R_P^2 values obtained by intra-particle diffusion kinetic model were not sufficiently high ($R^2 < 0.8821$) and had large intercept value, which confirmed that intra-particle diffusion was not the only rate limiting mechanism in the adsorption process. Values of C_P give an idea about the thickness of the boundary layer. By increasing boundary layer thickness, the contribution

Table 6 | The kinetic and isotherm equations used for the adsorption of reactive dyes onto CTS/MMT

Model type	Adsorption models	Equations
Kinetic models	Avrami fractionary order	$q_t = q_e\{1 - \exp[-(k_{Av}t)]^{n_{Av}}\}$
	Pseudo-first-order	$q_t = q_e[1 - \exp(-k_1 t)]$
	Pseudo-second-order	$q_t = \frac{q_e^2 k_2 t}{1 + q_e k_2 t}$
	Elovich	$q_t = \frac{1}{\beta}\ln(1 + \alpha\beta t)$
	Intra-particle diffusion	$q_t = k_p\sqrt{t} + C$
Isotherm models	Langmuir	$q_e = \frac{q_m K_L C_e}{1 + K_L C_e} \quad R_L = \frac{1}{1 + K_L C_0}$
	Freundlich	$q_e = K_F C_e^{1/n}$
	Dubinin-Radushkevich	$q_e = q_m \exp(-B_{DR}\varepsilon^2) \quad \varepsilon = RT\ln\left(1 + \frac{1}{C_e}\right) \quad E_{DR} = \frac{1}{\sqrt{2B_{DR}}}$
	Temkin	$q_e = \frac{RT}{b_T}\ln(A_T C_e)$
	Langmuir-Freundlich	$q_e = \frac{q_m (K_{LF} C_e)^m}{1 + (K_{LF} C_e)^m}$
	Sips	$q_e = \frac{q_m K_S C_e^{n_S}}{1 + K_S C_e^{n_S}}$
	Toth	$q_e = \frac{q_m C_e}{(1/K_T + C_e^t)^{1/t}}$

of the intra-particle diffusion model was declined, while that of the film diffusion model was increased (Kannan & Sundaram 2001). Compared with the four kinds of reactive dyes, RR136 adsorption had the largest C_P, attributed to the largest external mass transfer resistance during diffusion across the liquid film surrounding the adsorbent particle.

Thus, the results collected from the kinetic models indicated that the adsorption process of reactive dyes onto CTS/MMT was dominated by the combined effect of surface adsorption, boundary layer diffusion and intra-particle diffusion.

Adsorption isotherms

The parameters of equilibrium isotherm not only are crucial to understand the interaction between adsorbate and adsorbent, but provide some insight into the adsorption mechanism. The importance of obtaining the best-fit isotherm becomes more significant because as more applications are developed, more accurate and detailed isotherm descriptions are required for the design of adsorbent treatment systems. The Langmuir, Freundlich, Dubinin-Radushkevich, Temkin, Langmuir-Freundlich, Sips and Toth isotherms used in the present study are given in Table 6.

The theoretical parameters of isotherms along with R^2 and χ^2 are listed in Table 8. Compared with four kinds of two-parameter models, namely Langmuir, Freundlich, Dubinin-Radushkevich, and Temkin, the Langmuir isotherm models had the lowest χ^2 (<0.074) and highest R^2 (>0.9979). Langmuir isotherm suggests monolayer adsorption with no lateral interaction and steric hindrance between the adsorbed molecules. The results indicated that monolayer coverage of the adsorbate is the main adsorption mechanism due to homogeneous distribution of active sites on the surface of CTS/MMT. The low separation factor (R_L) values shown in Table 8 indicated that all the adsorption nature to be favorable and the interaction between dye molecules and CTS/MMT might be relatively strong.

The Freundlich isotherm is an empirical equation based on an exponential distribution of adsorption sites and energies. The values of $1/n$ imply the type of isotherm and can be classified as irreversible ($1/n = 0$), favorable ($1/n < 1$) and unfavorable ($1/n > 1$). The values of $1/n$ were found to be

Table 7 | Kinetic parameters by non linear method for the adsorption of reactive dyes onto CTS/MMT

		Reactive dye			
Kinetic model	**Parameters**	**RB5**	**RR136**	**RY145**	**RB222**
	$q_{e,exp}$	258.96	403.62	317.23	269.16
Avrami fractionary order	$q_{e,cal}$	250.06	395.74	311.15	265.66
	k_{Av}	0.031	0.045	0.038	0.029
	n_{Av}	0.750	0.682	0.695	0.740
	R^2	0.9998	0.9998	0.9996	0.9996
	χ^2	0.030	0.033	0.050	0.057
Pseudo-first-order	$q_{e,cal}$	237.07	377.51	294.44	250.15
	k_1	0.036	0.050	0.044	0.035
	R^2	0.9834	0.9701	0.9735	0.9813
	χ^2	3.761	6.689	5.608	4.510
Pseudo-second-order	$q_{e,cal}$	275.41	422.52	334.38	291.58
	$k_2 \times 10^4$	1.55	1.60	1.67	1.41
	R^2	0.9990	0.9984	0.9987	0.9989
	χ^2	0.162	0.225	0.190	0.190
Elovich	α	24.57	96.70	50.22	24.27
	β	0.0175	0.0137	0.0160	0.0163
	R^2	0.9711	0.9552	0.9660	0.9746
	χ^2	3.964	6.485	4.590	3.731
Intra-particle diffusion	k_p	13.34	17.40	14.86	14.29
	C_P	72.40	169.37	114.76	73.20
	R_P^2	0.8738	0.8314	0.8557	0.8821
	χ^2	18.657	25.671	20.667	18.826

Adsorption conditions: initial concentration of dyes 200 mg/L, adsorbent dosage 0.4 g/L, contact time 10–240 min, pH and temperature at the optimum condition as shown in Table 5.

less than 1, while the values of R_L for reactive dyes were obtained in the range 0–1, strongly supporting the favorable nature of the adsorption process.

The Dubinin-Radushkevich isotherm was used to estimate the apparent free energy of adsorption as well as to make a difference between the physical and the chemical adsorption process. The value of E_{DR} gives reliable information for predicting the mean energy of adsorption. If the value of E_{DR} is between 8 and 16 kJ/mol, the adsorption process follows the ion-exchange mechanism, while lower than 8 kJ/mol indicates a physical nature (Chao *et al.* 2014). The E_{DR} values shown in Table 8 revealed that reactive dyes are physically adsorbed on CTS/MMT.

Temkin isotherm assumes that adsorption is characterized by a uniform distribution of binding energy. The constant, b_T, is related to the mean free energy of adsorption per mole of the adsorbate as it is transferred to the surface of the adsorbent from an infinite distance in the solution. The magnitude of b_T for the ion-exchange mechanism was reported to be in the range of 8–16 kJ/mol, while the physisorption process was reported to have adsorption energies less than −40 kJ/mol (Kiran & Kaushik 2008). The very low values of b_T as shown in Table 8, range from 44.62 to 74.17 J/mol, indicated the reactive dyes removal involved physisorption.

Three-parameter isotherms, including Langmuir-Freundlich, Sips and Toth isotherm, were selected in this study. As shown in Table 8, as expected, versus two-parameter models, three-parameter isotherms all gave better fits due to $R^2 > 0.9990$ and $\chi^2 < 0.031$. The values of m_{LF} in Langmuir-Freundlich, n_s in Sips and t in Toth for all four kinds of reactive dyes tending to unity means that the adsorption data conformed to Langmuir model better than Freundlich model. The parameters m_{LF}, n_s and t also could be regarded as the parameters characterizing the system heterogeneity (Chatterjee *et al.* 2010). The three heterogeneity parameters are almost equal to unity and the order of dyes was RR136 > RY145 > RB222 > RB5, indicated the adsorption systems may be homogeneous and the condition is most homogeneous for RR136 (Grant & Phillips 1998). This information did not point out adsorbent structural property or the adsorbate property which is the reason of homogeneity or heterogeneity, but roughly pointed to the fact that the adsorbate property may be the most important reason because there is yet a considerable difference among the values of the heterogeneity parameters even when the same adsorbent was used (McKay *et al.* 2014).

The values of K_{LF} in Langmuir-Freundlich, K_s in Sips, and K_T in Toth could be regarded as the parameters characterizing the system affinity (Rill *et al.* 2009). The higher the value of the affinity parameter indicates the higher the adsorption affinity. As shown in Table 8, the highest affinity constant was obtained for the adsorption system of RB5, which is the lowest for RR136, and indicated that there are the strongest connections between RB5 molecules and the surface of CTS/MMT; desorption probability of this dye is lower than that for the other dyes.

Compared with three kinds of three-parameter models, in case of each dye, each isotherm model showed almost the same R^2 and χ^2. Thus, we assumed that this is the best isotherm model according to not only R^2 and χ^2, but Fractional Theoretical Capacity (FTC) measure. Of the

Table 8 | The values of parameters for each isotherm obtained by non linear regression for the experiment of reactive dyes adsorption onto CTS/MMT

		Reactive dye			
Isotherms	**Parameter**	**RB5**	**RR136**	**RY145**	**RB222**
Langumir	q_m	293.46	473.92	363.33	325.94
	K_{L}	0.103	0.099	0.101	0.102
	R^2	0.9979	0.9996	0.9996	0.9994
	χ^2	0.074	0.021	0.015	0.023
	R_{L}	0.024–0.163	0.025–0.168	0.024–0.165	0.024–0.163
Freundlich	K_{F}	130.55	204.66	159.42	143.95
	$1/n$	0.147	0.152	0.150	0.149
	R^2	0.9561	0.9466	0.9498	0.9521
	χ^2	1.610	3.372	2.337	1.953
Dubinin-Radushkevich	q_m	274.64	443.67	340.62	305.72
	B_{DR}	17.47	22.37	17.96	17.74
	E_{DR}	0.169	0.149	0.167	0.168
	R^2	0.9179	0.9426	0.9387	0.9344
	χ^2	3.062	3.734	2.952	2.793
Temkin	A_T	12.88	10.16	11.53	12.16
	b_T	74.17	44.62	59.10	66.31
	R^2	0.9733	0.9664	0.9686	0.9703
	χ^2	0.984	2.154	1.481	1.222
Langmuir-Freundlich	q_m	300.18	474.01	365.26	329.30
	K_{LF}	0.107	0.099	0.102	0.104
	m_{LF}	0.870	0.999	0.966	0.936
	R^2	0.9990	0.9996	0.9997	0.9997
	χ^2	0.031	0.021	0.012	0.012
Sips	q_m	300.18	474.01	365.27	329.85
	n_s	0.921	0.999	0.966	0.924
	K_s	0.143	0.099	0.111	0.124
	R^2	0.9990	0.9996	0.9997	0.9996
	χ^2	0.031	0.021	0.012	0.012
Toth	q_m	301.01	474.18	365.56	332.52
	K_{T}	0.188	0.100	0.120	0.168
	t	0.843	0.996	0.957	0.870
	R^2	0.9990	0.9996	0.9997	0.9995
	χ^2	0.031	0.021	0.012	0.018

Adsorption conditions: initial dye concentration range 50–400 mg/L, adsorbent dosage 0.4 g/L, contact time 240 min, pH and temperature at the optimum condition as shown in Table 5.

isotherm models based on FTC, the best will be the model which has the highest predicted adsorption capacity (McKay *et al.* 2014). As shown in Table 8, in all selected isotherm models, Toth model is the best model for the description of the experimental data of all studied dye and CTS/MMT systems in this study.

Thermodynamic studies

Thermodynamic parameters provide further information about inherent energetic changes associated with the adsorption process. The thermodynamic parameters are listed in Table 9. The negative ΔG^{o} values were obtained

Table 9 | Thermodynamic parameters for adsorption of reactive dyes onto CTS/MMT

	ΔG^o (kJ/mol)						$T\Delta S^o$ (kJ/mol)			
Reactive dye	**293 K**	**303 K**	**313 K**	**323 K**	ΔH^o (kJ/mol)	ΔS^o (J/(mol K))	**293 K**	**303 K**	**313 K**	**323 K**
RB5	−6.58	−7.48	−8.44	−9.30	20.24	91.52	26.81	27.73	28.64	29.56
RR136	−9.50	−9.34	−9.08	−8.69	−17.36	−26.64	−7.80	−8.07	−8.34	−8.60
RY145	−7.46	−8.16	−8.89	−9.84	15.52	78.26	22.93	23.71	24.50	25.28
RB222	−7.04	−7.79	−8.62	−9.58	17.62	84.03	24.62	25.46	26.30	27.14

in all investigated temperature range, revealing the feasible and spontaneous adsorption processes for four kinds of reactive dyes onto CTS/MMT (Jethave *et al.* 2017). The adsorption process of RR136 showed that the highest negative value indicated most energetically favorable adsorption.

In the cases of RB5, RY145 and RB222, the ΔH^o values were found to be positive which confirmed endothermic adsorption (Ceglowski & Schroeder 2015). The endothermic process was due to the enhancement of diffusion rate of the dye molecules across the external boundary layer and in the internal of CTS/MMT. The negative value of ΔH^o indicated that the adsorption of RR136 onto CTS/MMT is exothermic. This exothermic process was attributed to the weakening of adsorptive forces between the binding sites and the dye species, and between the adjacent dye molecules on the adsorbed phase. Besides, higher temperature may enhance the solubility and desorption of RR136, hence the solute molecules were more difficult adsorb. The small values of ΔH^o ($|\Delta H^o| < 20.24$ kJ/mol) for four kinds of reactive dyes were not compatible with the formation of strong chemical bonds between the dye molecules and CTS/MMT, and the adsorption process was likely to be due to weak electrostatic interactions (Kara *et al.* 2003).

The positive ΔS^o for RB5, RY145 and RB222 indicated an increase in the level of disorder of the adsorbed species and suggested the possibility of some structural changes or readjustments in the dye-adsorbent adsorption complex (Song *et al.* 2016). The negative value of ΔS^o for RR136 meant decreased randomness at the solid–solution interface during adsorption, which may be caused by the restricted mobility of reactive dyes on the surface of CTS/MMT compared with that of aqueous solution and no significant change occurs in the internal structure of the adsorbent during the adsorption process. The data given in Table 9 showed that $|\Delta H^o| < |T\Delta S^o|$ for RB5, RY145 and RB222, which indicated that the adsorption process is dominated by entropic rather than enthalpic changes, while the adsorption process of RR136 is dominated by enthalpic changes.

CONCLUSION

Taguchi-GRA method was employed to optimize the adsorption process of reactive dyes onto chitosan intercalated montmorillonite composite considering the simultaneous influence of five operational variables such as pH value, dyes concentration, temperature, adsorbent dosage and contact time, each at four different levels. Taguchi-GRA method gave a suitable approach to determination optimal combination adsorption conditions for simultaneous maximization of R% and q. The optimal adsorption conditions were found in pH 3, initial concentration of dye 300 mg/L, temperature 50 °C, adsorbent dosage 0.7 g/L and contact time 240 min for RB5 and RY145; pH 3, initial concentration of dye 200 mg/L, temperature 20 °C, adsorbent dosage 0.5 g/L and contact time 180 min for RR136; pH 3, initial concentration of dye 100 mg/L, temperature 50 °C, adsorbent dosage 0.4 g/L and contact time 240 min for RB222. The experimental and predicted response matched each other. The kinetic of reactive dyes adsorption followed the Avrami fractionary order expression and was well described by the Toth isotherm model. The adsorption process of reactive dyes onto CTS/MMT indicated that adsorption was dominated by the combined effect of surface adsorption, boundary layer diffusion and intra-particle diffusion. The thermodynamic estimates indicated feasibility and spontaneous nature of the adsorption, while endothermic for RB5, RY145 and RB222, and exothermic for RR136. The obtained results show that CTS/MMT is an efficient low-cost adsorbent for reactive dyes and has a high potential of the sorbent to remove other color contaminants.

ACKNOWLEDGEMENTS

This work was financially supported by the National Natural Science Foundation of China (41106067), Natural Science Foundation of Shandong Province (ZR2010BQ013), Applied

Basic Research Project of Qingdao City (13-1-4-252-jch), PR China, and the Open Project Program for Key Laboratory of Fermentation Engineering (Ministry of Education).

REFERENCES

Alexandre, M. & Dubois, P. 2000 Polymer-layered silicate nanocomposites: preparation, properties and uses of a new class of materials. *Materials Science & Engineering, R: Reports* **28** (1–2), 1–63.

Blackburn, R. S. 2004 Natural polysaccharides and their interactions with dye molecules: applications in effluent treatment. *Environmental Science & Technology* **38** (18), 4905–4909.

Boparai, H. K., Joseph, M. & O'Carroll, D. M. 2011 Kinetics and thermodynamics of cadmium ion removal by adsorption onto nano zerovalent iron particles. *Journal of Hazardous Materials* **186** (1), 458–465.

Ceglowski, M. A. & Schroeder, G. 2015 Removal of heavy metal ions with the use of chelating polymers obtained by grafting pyridine-pyrazole ligands onto polymethylhydrosiloxane. *Chemical Engineering Journal* **259**, 885–893.

Cestari, A. R., Vieira, E. F. S., Vleira, G. S. & Almeida, L. E. 2006 The removal of anionic dyes from aqueous solutions in the presence of anionic surfactant using aminopropylsilica – A kinetic study. *Journal of Hazardous Materials* **138** (1), 133–141.

Chao, Y., Zhu, W., Wu, X., Hou, F., Xun, S., Wu, P., Ji, H., Xu, H. & Li, H. 2014 Application of graphene-like layered molybdenum disulfide and its excellent adsorption behavior for doxycycline antibiotic. *Chemical Engineering Journal* **243** (5), 60–67.

Chatterjee, S., Lee, M. W. & Woo, S. H. 2010 Adsorption of congo red by chitosan hydrogel beads impregnated with carbon nanotubes. *Bioresource Technology* **101** (6), 1800–1806.

Grant, P. G. & Phillips, T. D. 1998 Isothermal adsorption of aflatoxin B-1 on HSCAS clay. *Journal of Agricultural and Food Chemistry* **46** (2), 599–605.

Ho, Y. S. & McKay, G. A. 1998 A comparison of chemisorption kinetic models applied to pollutant removal on various sorbents. *Process Safety and Environmental Protection* **76** (4), 332–340.

Ho, Y. S. & McKay, G. 1999 Pseudo-second-order model for sorption processes. *Process Biochemistry* **34** (5), 451–465.

Jethave, G., Fegade, U., Attarde, S. & Ingle, S. 2017 Facile synthesis of lead doped zinc-aluminum oxide nanoparticles (LD-ZAO-NPs) for efficient adsorption of anionic dye: kinetic, isotherm and thermodynamic behaviors. *Journal of Industrial and Engineering Chemistry* **53**, 294–306.

Kannan, N. & Sundaram, M. M. 2001 Kinetics and mechanism of removal of methylene blue by adsorption on various carbons-a comparative study. *Dyes and Pigments* **51** (1), 25–40.

Kara, M., Yuzer, H., Sabah, E. & Celik, M. S. 2003 Adsorption of cobalt from aqueous solutions onto sepiolite. *Water Research* **37** (1), 224–232.

Kiran, B. & Kaushik, A. 2008 Chromium binding capacity of *Lyngbya putealis* exopolysaccharides. *Biochemical Engineering Journal* **38** (1), 47–54.

Liang, X., Xu, Y., Wang, L., Sun, Y., Lin, D., Sun, Y., Qin, X. & Wan, Q. 2013 Sorption of Pb^{2+} on mercapto functionalized sepiolite. *Chemosphere* **90** (2), 548–555.

Lopes, E. C., dos Anjos, F. S., Vieira, E. F. & Cestari, A. R. 2003 An alternative Avrami equation to evaluate kinetic parameters of the interaction of Hg(II) with thin chitosan membranes. *Journal of Colloid and Interface Science* **263** (2), 542–547.

McKay, G., Mesdaghinia, A., Nassert, S., Hadi, M. & Aminabad, M. S. 2014 Optimum isotherms of dyes sorption by activated carbon: fractional theoretical capacity & error analysis. *Chemical Engineering Journal* **251**, 236–247.

Monvisade, P. & Siriphannon, P. 2009 Chitosan intercalated montmorillonite: preparation, characterization and cationic dye adsorption. *Applied Clay Science* **42** (3), 427–431.

Oliveira, G. A. R., Ferraz, E. R. A., Leme, D. M., Zanoni, M. V. B., Li, Z., Urban, J. & Oliveira, D. P. 2011 Assays of cytotoxicity and mutagenicity as a tool for assessment of consumer exposed to textile dyes. *Toxicology Letters* **205** (12), S107.

Rill, C., Kolar, Z. I., Kickelbick, G., Wolterbeek, H. T. & Peters, J. A. 2009 Kinetics and thermodynamics of adsorption on hydroxyapatite of the [^{160}Tb] Terbium complexes of the bone-targeting ligands DOTP and BPPED. *Langmuir* **25** (4), 2294–2301.

Song, W., Gao, B., Xu, X., Xing, L., Han, S., Duan, P., Song, W. & Jia, R. 2016 Adsorption-desorption behavior of magnetic amine/Fe_3O_4 funcitonalized biopolymer resin towards anionic dyes from wastewater. *Bioresource Technology* **210**, 123–130.

Wang, L., Zhang, J. & Wang, A. 2008 Removal of methylene blue from aqueous solution using chitosan-g-poly(acrylic acid)/montmorillonite superadsorbent nanocomposite. *Colloids and Surfaces, A: Physicochemical and Engineering Aspects* **322** (1–3), 47–53.

Zhao, P., Zhang, R. & Wang, J. 2017 Adsorption of methyl orange from aqueous solution using chitosan/diatomite composite. *Water Science and Technology* **75** (7), 1633–1642.

Zolgharnein, J., Asanjarani, N. & Shariatmanesh, T. 2013 Taguchi L_{16} orthogonal array optimization for Cd(II) removal using *Carpinus betulus* tree leaves: adsorption characterization. *International Biodeterioration & Biodegradation* **85**, 66–77.

Zolgharnein, J., Asanjrani, N., Bagtash, M. & Azimi, G. 2014 Multi-response optimization using Taguchi design and principle component analysis for removing binary mixture of alizarin red and alizarin yellow from aqueous solution by nano gamma-alumina. *Spectrochimica Acta, Part A: Molecular and Biomolecular Spectroscopy* **126** (6), 291–300.

First received 6 March 2018; accepted in revised form 4 May 2018. Available online 15 May 2018